Effect of FEM Domain on the Estimation of the Bearing Capacity Factor of Sand

Teachavorasinskun Supot
Lecturer, Department of Civil Engineering, Faculty of Engineering,
Chulalongkorn University, Phayathai Rd., Pathumwan, Bangkok 10330, Thailand.
E-mail : tsupot@chula.ac.th

Pongvithayapanu Pulpong
Graduate student, Sirindhorn International Institute of Technology,
Thammasat University, Rangsit Campus, Pathumthani, Thailand.
E-mail : pulpong@hotmail.com

Abstract

A finite element analysis program was employed to simulate the load bearing characteristic of the assumed FEM domains. The elastic-perfectly plastic model; i.e., Drucker-Prager model, was used to represent the constitutive relationship of sand. Three analytical cases were carried out to investigate the bearing capacity characteristic of an ideal sand. The first analysis case was done by adding some additional meshes to the typical FEM domain (*ADD case*). The results indicated an indiscernible change on the ultimate bearing capacity computed using the typical and *ADD case* domains. However, if the unit length of the typical FEM domain was multiplied by a scalar factor (*ADJUST case*), the computed bearing capacity factor became higher than that obtained from *ADD case* having similar boundary condition. Finally, the effect of acceleration field was investigated by changing the unit weight of the material (*ng case*). The bearing capacity factor obtained from the *ng case* was smaller than that obtained from the *1g case* having similar FEM domain and footing width. When the apparent footing width was used for the purpose of comparison, the deviation between *1g* and *ng* simulations became smaller, especially when larger footing was employed.

1. Introduction

Model testing has been a popular tool in the determination of the bearing capacity of soil. The usage of the so-called *1g* model test limits the study to cover only a small size footing due mostly to the cost effectiveness. As a result, reasonable links have been established to extend *1g* test results to estimate the bearing capacity of the prototype footing [1,2,3,4]. The development of the centrifugal equipment allows the researchers to master this limitation and plays a very important role in verification of the existing links between model and prototype footings.

For footing resting on the surface of sand, the ultimate bearing capacity could be simply written as a function of the bearing capacity factor, N_γ, as;

$$q_{ult} = \frac{(n\gamma)B_0}{2} N_\gamma \qquad (1)$$

where B_0 is the width of model footing, n is the ratio of the acceleration field to the gravitational acceleration, g, and γ is the unit weight of sand under gravitational acceleration. Eqn.(1) is usually interpreted so that the factor n is used to multiply to the parameter B_0 and results in the apparent footing width, B_{app} as expressed by;

$$B_{app} = nB_0 = B_{pro} \qquad (2)$$

By applying large values of n, the effects footing width can be investigated using small model box. Tatsuoka et al. [3] reported the difference between the bearing capacity factor, N_γ, obtained from the *1g* and *ng* model tests as reproduced in Fig.1. The *ng* test tends to give higher values of the bearing capacity factor as the apparent width of footing increases. They believed that the deviation was due to the effect of particle size.

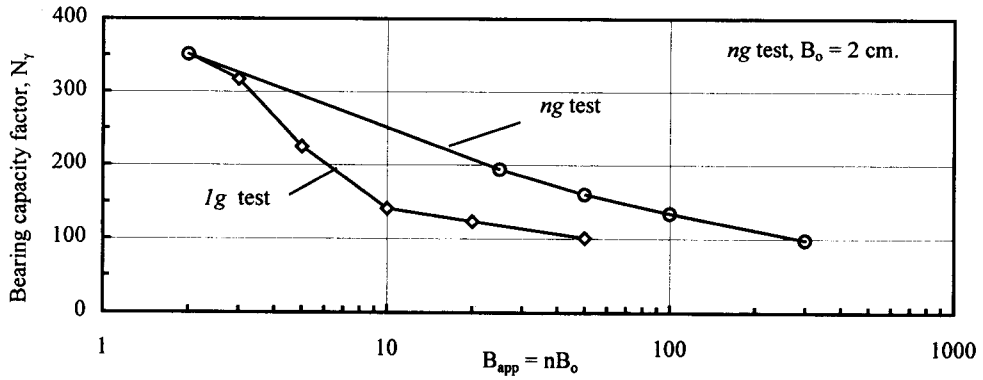

Fig.1 Comparison between the *1g* and *ng* test results (from Tatsuoka et al.(1991))

Fig.2 shows schematically the difference in overburden pressure distribution in the model soil under *1g* and *ng* tests. The stress bulb is assumed to be dependent only on the footing width, B_0. Therefore, the overburden stress of the soil mass bounded by the stress bulb in *ng*

test (Fig. 2(b)) is supposedly n times greater than that in the *1g* test (Fig.2(a)). The increase in the bearing capacity observed in *ng* test is mostly due to this stress difference. Fig. 2(d) shows one and most popular interpretation of *ng* test; i.e., the ideal prototype model. In this case, the initial stress in the zone bounded by the stress bulb could be similar to that shown in Fig.2(b). Fig.2(c) shows another way of interpretation of *ng* test. It is clear that this is an incomplete interpretation. It could be seen that under *ng* test, soil beneath the footing is subjected to very high stress intensity. In other words, if the finite element approximation is used to verify the case, the FEM domain; i.e., mesh densities, should be properly adjusted according to the applied acceleration to obtain the most reliable result.

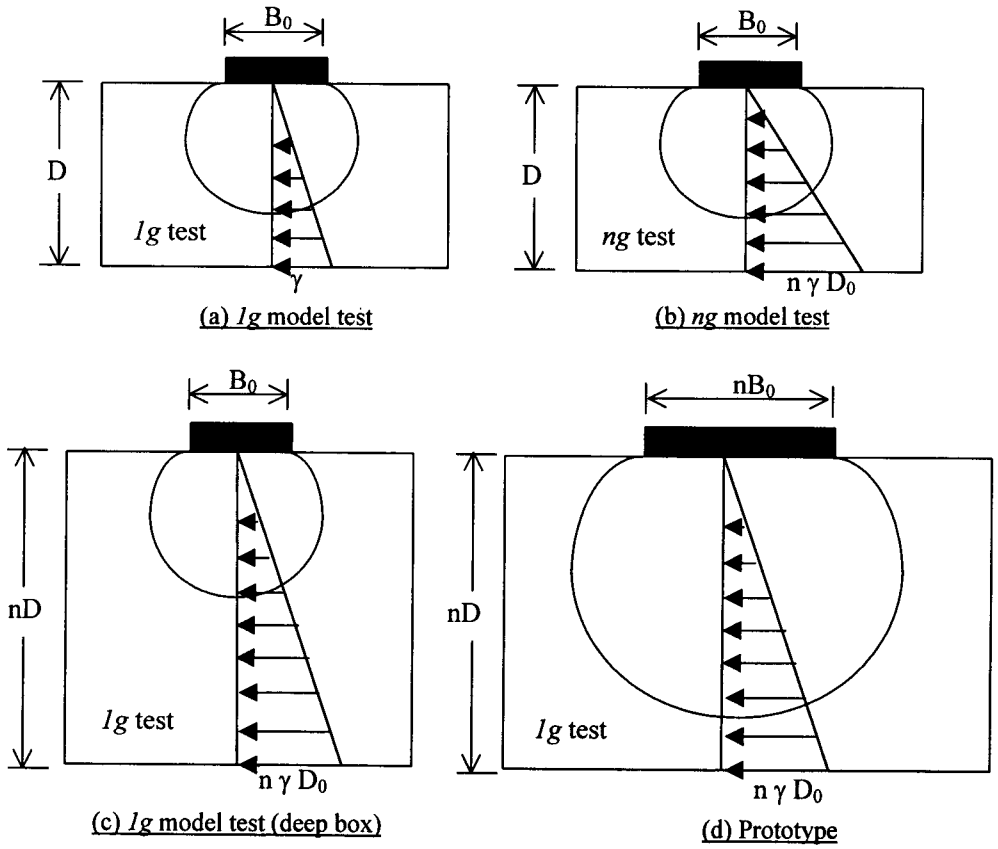

Fig. 2 Schematic comparison among the *1g*, *ng* and prototype tests.

In the present study, the FEM domain used in the FEM analysis was manipulated to investigate its effects on the computed bearing capacity. Adjustment of FEM mesh was done on

the typical mesh (Fig.3(a)) which was used as reference. Two types of modified meshes were used; i.e., the *ADJUST* (Fig.2 (b)) and *ADD* (Fig.2 (c)) cases. Furthermore, in some analytical cases under high stress intensity, the mesh density beneath the footing was increased to see its effect on FEM approximation.

2. Effects of footing width on the bearing capacity of sand

Fig.4 shows the plots between the bearing capacity factor, N_γ, and the settlement ratio, Δ/B_0, of the node beneath the center of the footing from several *ADD* cases. As could be expected, the effect of the FEM domain formed on the load bearing characteristic is indiscernible. On the contrary, the results obtained from the *ADJUST* case exhibit strong dependency of bearing capacity on the FEM domain as can be seen in Fig.5. The FEM domains used in the *ADJUST* cases were much coarser than the typical one and result in larger error in FEM approximation. The values of the maximum bearing capacity factor, $(N_\gamma)_{max}$, for *ADD* case are summarized in Table 1 and plotted against the footing width, B_0, in Fig.6. It is clear from the figure that $(N_\gamma)_{max}$ decreases as the footing width increases. This tendency corresponds well to test results presented in the literature (Fig.1).

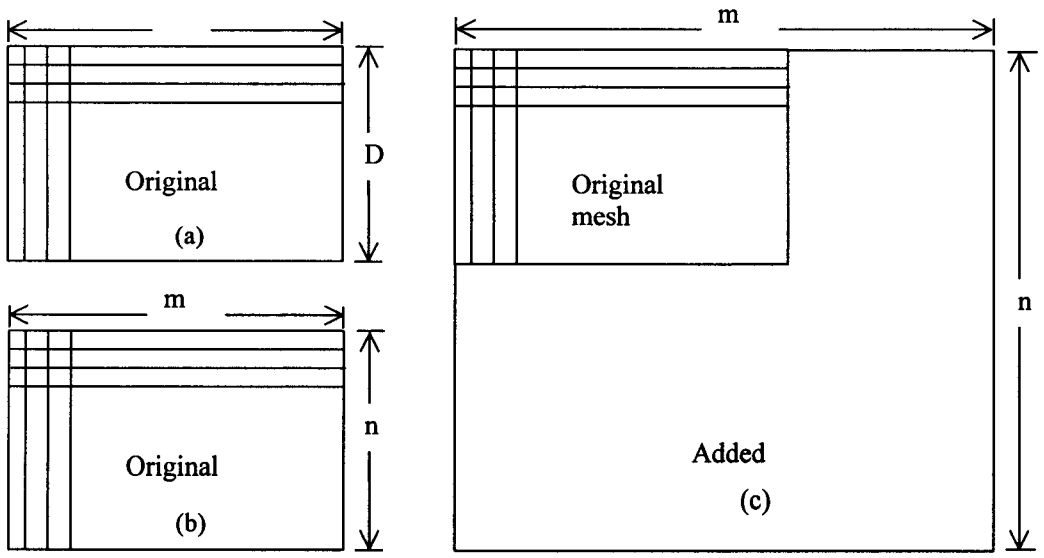

Fig. 3 FEM mesh arrangements (a) typical mesh, (b) *ADJUST* case and (c) *ADD* case

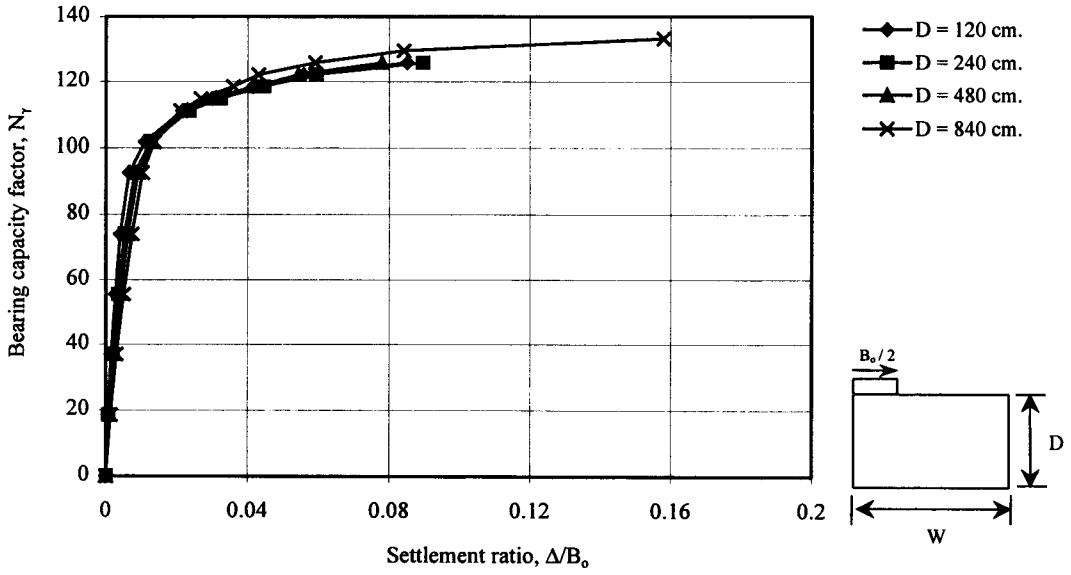

Fig.4 Load bearing characteristic of 30 cm. width of footing from *ADD* case

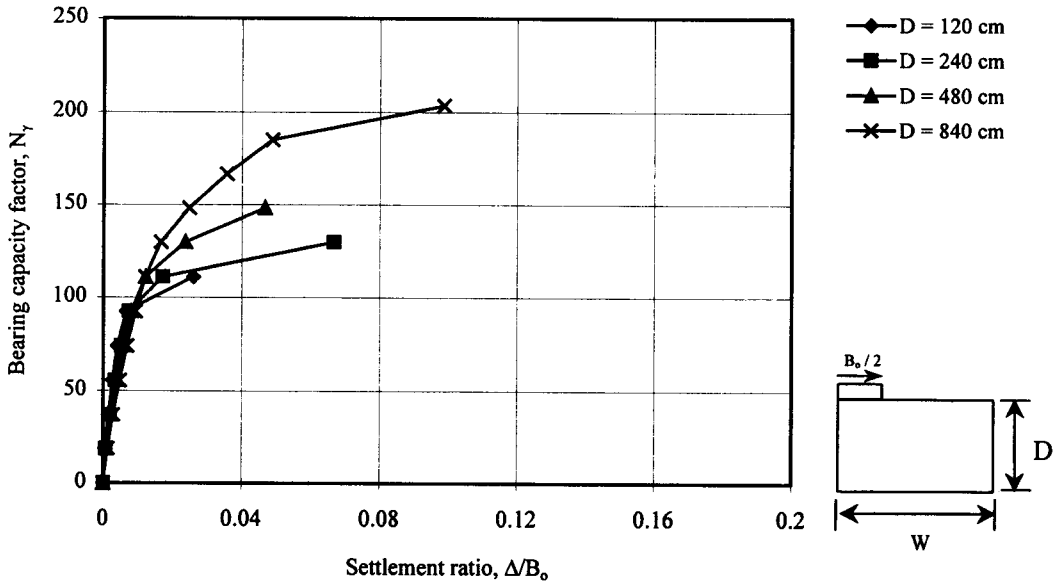

Fig.5 Load bearing characteristic of 30 cm. width of footing from *ADJUST* case

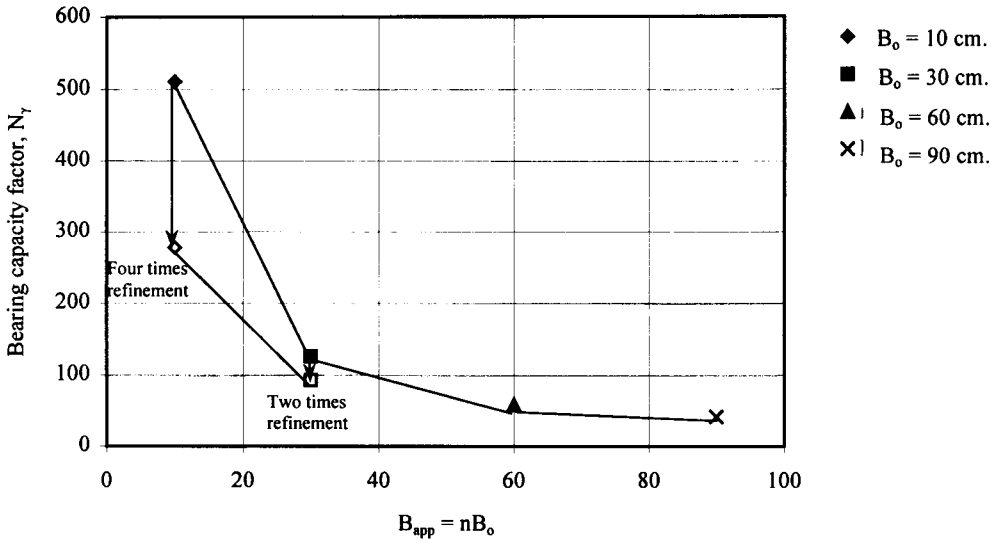

Fig.6 Comparison of $(N_\gamma)_{max}$ obtained with four different footing widths (*1g* simulation)

The $(N_\gamma)_{max}$ obtained from *ng*-simulation using the typical domain with different footing widths are shown in Fig.7. For the case when B_0 = 30, 60 and 90 cm, the simulation when $n < 1g$ was also carried out. Note that the apparent footing width (Eq. (2)) is used in plotting the results of *ng* simulation. The effect of acceleration field is dependent on the size of the footing. Namely, when the footing width, B_0, is small (i.e., B_0 = 10 and 30 cm), the difference between *1g* and *ng* is very obvious. However, as the footing width increases, the difference becomes smaller. The usual widths of footing used in the actual centrifugal test was about 2-3 cm [3,4,5] which is very small. And, as deduced from the result of the present study, the difference between the *1g* and *ng* test results should be very large as reported in the literature (Fig.1). To be sure that this is not the effect of boundary presumed in the FEM domains, some *ng* simulations were carried out using the *ADD* case meshes as shown in Table 2. It can be seen that there is no effect of the presumed boundary on the computed results.

Table 1 $(N_\gamma)_{max}$ computed from *ADD* case (*1g* simulation)

	Bearing capacity factor, N_γ								
	B_o = 30 cm			B_o = 60 cm.			B_o = 90 cm.		
	W=240 cm.	W=360 cm.	W=720 cm.	W=240 cm.	W=360 cm.	W=720 cm.	W=240 cm.	W=360 cm.	W=720 cm.
D = 120 cm.	126	126	126	59	61	61	42	42	42
D = 240 cm.	126	126	126	57	59	61	41	40	41
D = 480 cm.	126	130	133	61	61	63	42	41	42
D = 840 cm.	133	133	137	63	63	65	44	42	43

Table 2 $(N_\gamma)_{max}$ from *ng* simulation (both typical domain and *ADD* domain)

		Bearing capacity factor, N_γ							
		n = 0.25	n = 0.5	n = 1	n = 1.75	n = 2	n = 3.5	n = 4	n = 7
W = 240	D = 120 cm.	-	-	126	-	72	-	44	30
B_o = 30 cm.	D = 240 cm.	-	230	126	-	72	49	-	30
	D = 480 cm.	407	230	126	83	-	-	-	-
W = 240	D = 120 cm.	-	-	59	-	35	-	22	15
B_o = 60 cm.	D = 240 cm.	-	102	57	-	35	24	-	-
	D = 480 cm.	185	111	61	36	-	-	-	-
W = 240	D = 120 cm.	-	-	42	-	25	-	15	10
B_o = 90 cm.	D = 240 cm.	-	68	41	-	25	17	-	-
	D = 480 cm.	123	68	42	28	-	-	-	-

3. Refinement of FEM domain

As the acceleration field increases, the stress intensity in each element also increases. The reliability of the FEM approximation is, therefore, subjected to question. Fig. 8 shows the effect of mesh density beneath the footing width on the $N_\gamma \sim \Delta/B_0$ relationships from the *ng* simulation. The mesh density in the vicinity of footing was twice increased. Some reduction in load bearing capacity of the domain can be observed, especially when high acceleration field is employed. Figs. 9 and 10 show the effect of mesh density on the bearing capacity characteristics of the *ng* simulations using the footing widths of 10 and 30 cm, respectively. It can be seen that further refinement does affect the bearing capacity characteristic of the assumed footing. The decrease in N_γ is very clear. It could be noted that if the value of N_γ obtained from the more refined mesh was used to plot the relationship in Fig. 7, a unique relationship between the $N_\gamma \sim B_{app}$ could be formed because of the nature of the Drucker-Prager model adopted in the computation.

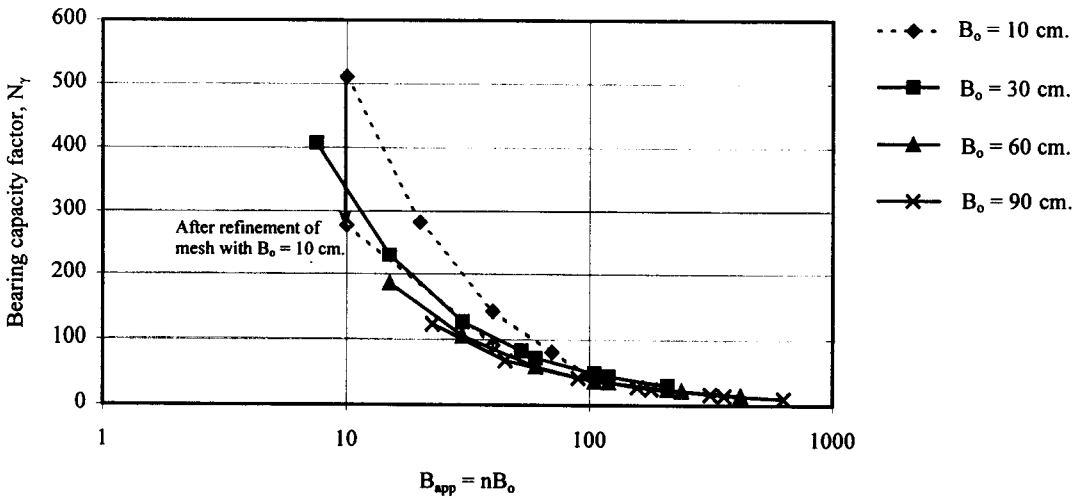

Fig. 7 Comparison between the *1g* and *ng* simulations

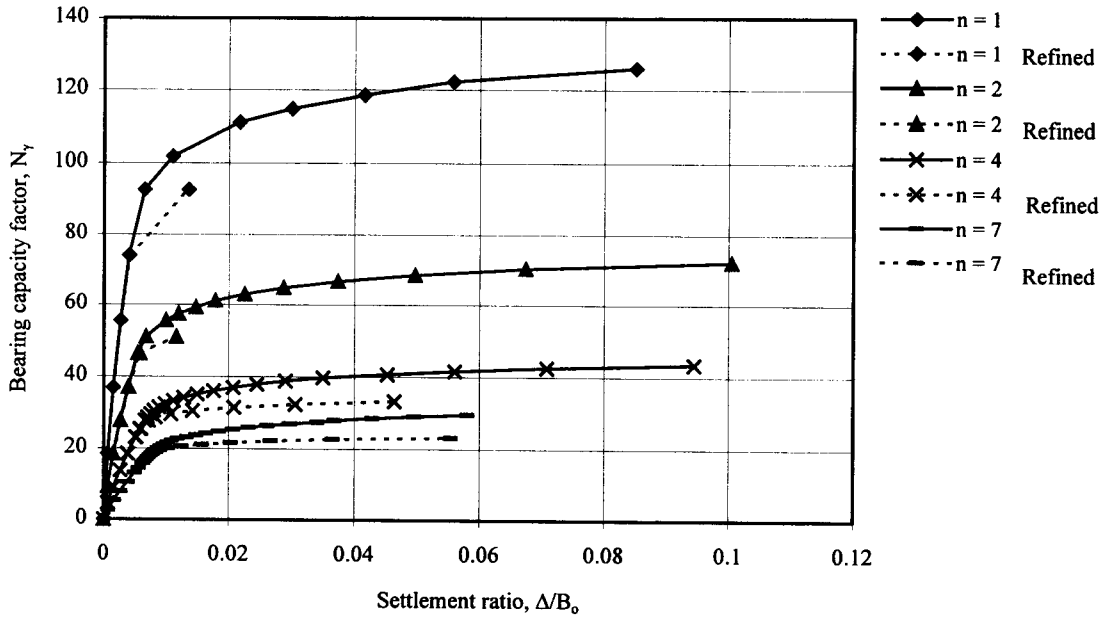

Fig. 8 Two times refinement of the typical mesh of B_o = 30 cm. at various acceleration fields

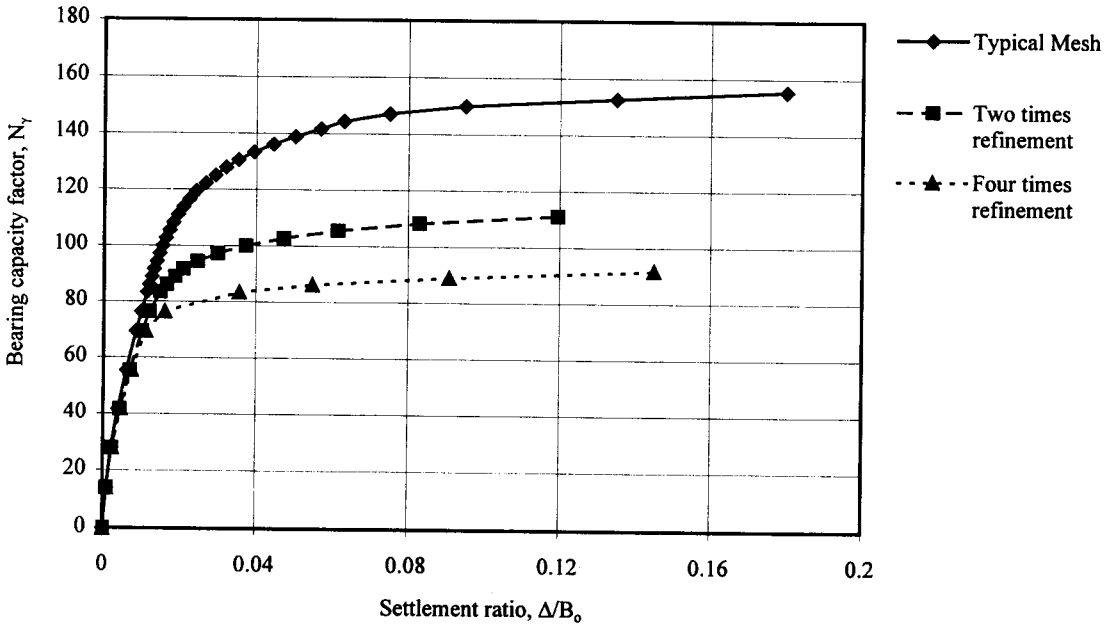

Fig. 9 Two and Four times refinement of the typical mesh of *ng* simulation at B_o=10 cm., n=4

4. Conclusions

The *1g* and *ng* simulations were carried out using the FEM analysis. It was found that the mesh density affected the computed bearing capacity characteristic. With the symmetric material model such as the Drucker-Prager model used in the present study, the difference between *1g* and *ng* simulations could be very small if proper mesh density was employed.

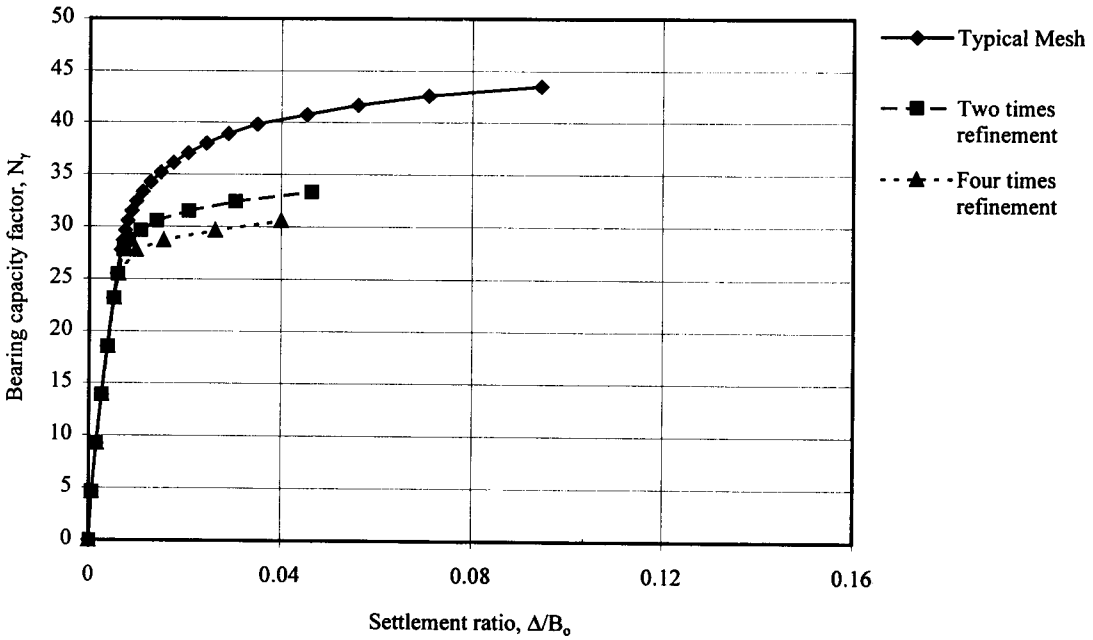

Fig. 10 Two and Four times refinement of the typical mesh of *ng* simulation at B_o=30 cm., n=4

5. References

[1] Vesic, A. S.(1973), Analysis of Ultimate Load of Shallow Foundations, Journal of Soil Mechanics and Foundations Division, ASCE, Vol.99, No.SM1, pp.45-73.

[2] Yamaguchi, H. Kimura, T. and Fujii, N. (1977),On the Scale Effects of Footings in Dense Sand, Proceeding of the 9th International Conference on Soil Mechanics and Foundation Engineering, Vol.1, pp.795-798.

[3] Tatsuoka, F., Okahara, M., Tanaka, T., Tani, K., Morimoto, T. and Siddiquee, M. S. A.(1991), Progressive Failure and Particle Size Effect in Bearing Capacity of Footing on Sand, Proceeding of the ASCE Geotechnical Engineering Congress, Boulder, Vol.1, pp.788-802.

[4] Kusakabe, O., Maeda, Y. and Ohuchi, M. (1992), Large-scale Loading Tests of Shallow Footings in Pneumatic Caisson, Journal of the Geotechnical Engineering, ASCE, Vol.118, No.11, pp.1681-1695.

[5] Aiban, A. S. and Znidarcic, D. (1996), Centrifugal Modeling of Bearing Capacity of Shallow Foundation on Sands, Journal of the Geotechnical Engineering, ASCE, Vol.121, No.10, pp.704-712.